Educational Administration: Theory and Practice
2024, 30(5), 10772 - 10786
ISSN: 2148-2403
https://kuey.net/

Research Article

Degradative Investigation Of Zinc Salt Of Poly(Ethylene-Co-Methacrylic Acid) Compatibilized LDPE-Starch Blends With Metal Oxide Pro-Oxidants

Zeena P. Hamza[1*], Anna Dilfi K. F.[2], Thomas Kurian[3]

[1*]Postgraduate and Research Department of Chemistry, Maharaja's College, Ernakulam, Kerala, India, 682011, *Emails: zeenaphamza@maharajas.ac.in, zeenaphamza@gmail.com
[2]Department of Chemistry, St. Xavier's College for Women, Aluva, Kerala, India, 683101
[3]Department of Polymer Science and Rubber Technology, Cochin University of Science and Technology, Kochi, Kerala, India, 682022

Citation: Zeena P. Hamza, et al (2024) Degradative Investigation Of Zinc Salt Of Poly(Ethylene-Co-Methacrylic Acid) Compatibilized LDPE-Starch Blends With Metal Oxide Pro-Oxidants", *Educational Administration: Theory and Practice*, *30*(5), 10772 - 10786
Doi: 10.53555/kuey.v30i5.4835

ARTICLE INFO

ABSTRACT

Metal oxides (iron oxide, manganese dioxide, titanium dioxide (anatase and rutile grades)) in various compositions (0.5 and 1 weight%) were added into EMA-Zn (5%) compatibilized low density polyethylene-starch blends. Mechanical properties, melt flow indices, biodegradability, photodegradability, photobiodegradability, water absorption, infrared spectroscopy, dynamic mechanical analysis, thermogravimetry, differential scanning calorimetry, and scanning electron microscopy were used to assess the role of small amounts of metal oxides as pro-oxidants in the blends. With the addition of metal oxides, the mechanical characteristics of the mixes changed. Thermal characterization using TGA and DSC revealed that the addition of metal oxides changed the thermal stability and crystallinity. Various degradative investigations suggest that the inclusion of metal oxides improves the blends' degradability.

Keywords: pro-oxidant, ionomer, metal oxide, biodegradability, photodegradability, photobiodegradability

1. INTRODUCTION

Oxo-biodegradation of polymers used in packaging applications is gaining popularity these days. Low density polyethylene is a popular polyolefin polymer for packaging purposes. To overcome low density polyethylene's inherent resistance to biological attack, two major strategies have been developed: (i) the incorporation of functional groups into the polyethylene backbone, and (ii) the blending of polyethylene with photo initiating pro-oxidants capable of promoting the formation of free radical precursor moieties by photo-oxidation to induce cleavage of the macromolecular backbone [Burelo, 2023; Zhang et al, 2022; Sanniyasi, 2021; Ammala et al, 2011].

Photo-oxidation of pro-oxidant-containing low density polyethylene-starch blends increases the low molecular weight fraction by chain scission, increasing biodegradation [Ghatge et al, 2020; Jiang et al, 2020; Inceoglu and Menceloglu, 2013]. It also increases the surface area due to embrittlement and subsequent track development. Furthermore, the development of carbonyl groups on the surface boosts polyethylene's hydrophilicity [Ali et al, 2018]. It has been reported that transition metals are good photoinitiators for polyethylene [Roy et al, 2006]. Because transition metals, particularly iron and manganese, have a remarkable ability to breakdown the hydroperoxides generated during the oxidation process of polymers, they are included in the majority of commercial photodegradable compositions [Bonhomme et al, 2003; Zhao et al, 2007; Bardaji et al, 2020]. TiO_2 has become a popular photocatalyst due to its excellent properties such as low cost, non-toxicity, stability, and strong photoactivity [Nagwan et al, 2020; Buchanan and Gibbons 1974].

This study investigates the use of metal oxides, specifically ferric oxide, manganese dioxide, and titanium dioxide (anatase and rutile grades), to improve the degradative qualities of EMA-Zn compatibilized low density polyethylene-starch blends. Table 1 shows the sample designations and descriptions utilized in this work. Mechanical properties, infrared spectroscopy, thermal properties, and scanning electron microscopy were used to characterize the films. The films' biodegradability, photodegradability, and photobiodegradability were also tested.

Table 1. Description of sample designations

Sample designation	Description
LDS-Zn	LDPE-20% starch-5% (EMA-Zn)
LDS-Zn-Fe	LDPE-20% starch-5% (EMA-Zn)-Fe_2O_3
LDS-Zn-Mn	LDPE-20% starch-5% (EMA-Zn)-MnO_2
LDS-Zn-Ru	LDPE-20% starch-5% (EMA-Zn)-TiO_2(rutile)
LDS-Zn-An	LDPE-20% starch-5% (EMA-Zn)- TiO_2(anatase)
LDS-Na	LDPE-20% starch-5% (EMA-Na)
LDS-Na-Fe	LDPE-20% starch-5% (EMA-Na)-Fe_2O_3
LDS-Na-Mn	LDPE-20% starch-5% (EMA-Na)-MnO_2
LDS-Na-Ru	LDPE-20% starch-5% (EMA-Na)-TiO_2(rutile)
LDS-Na-An	LDPE-20% starch-5% (EMA-Na)- TiO_2(anatase)

2. EXPERIMENTS AND METHODS

2.1 Materials

2.1.1 Low density polyethylene (LDPE)

The film grade low density polyethylene (LDPE 24FS040) from Reliance Industries Limited, Mumbai, India, with melt flow index (190 °C/2.16 kg) of 4 g/10 min and density (23 °C) of 0.922 g/cm^3 was supplied by Periyar Polyfilms, Edayar, Kerala, India.

2.1.2 Starch

The tapioca starch (100 and 300 mesh) was obtained from Jemsons Starch & Derivatives, Aroor, Alappuzha, Kerala. As these fillers were hygroscopic in nature they were oven dried at 120 °C for 1h prior to mixing.

2.1.3 Ionomers

Ionomer used in this study was Zinc salt of poly(ethylene-co-methacrylic acid) (HIMILAN 1702 EMAAZn) with melt flow index (190 °C/2.16 kg) of 16 g/10 min.
These ionomers were supplied by Mitsubishi Plastics, Inc., Japan.

2.1.4 Pro-oxidants

Metal oxides such as iron oxide, manganese dioxide, and titanium dioxide (anatase and rutile grades) were used as pro-oxidants in this study. Merck Specialities Pvt. Ltd., Mumbai, India, supplied the iron oxide. Qualigens Fine Chemicals, Mumbai, India, supplied the manganese dioxide. Associated Chemicals, Edappally, Kerala, India, supplied titanium dioxide (anatase and rutile grades).

2.2 Methods

2.2.1 Preparation of blends

Blends were prepared by melt mixing method because it is:

- environmentally benign
- suitable for most of the polymers
- compatible with practicing polymer processing operations
- the most popular method for industrial applications

A Thermo Haake Polylab system (Rheocord 600p) equipped with roller-type rotors was used for melt mixing. The mixing chamber has a volumetric capacity of 69 cm^3. A mixing time of 8 minutes was given for all the compounds at a rotor speed of 30 rpm at 150 °C. LDPE together with ionomer was first melted for 2 minutes followed by the addition of filler. Mixing was continued for another 6 minutes.

2.2.2 Preparation of test specimens

The test specimens were prepared from neat LDPE and the compounds by moulding in an electrically heated hydraulic press for 5 minutes at 150 °C under a pressure of 20 MPa. After moulding, the samples were cooled down to room temperature under pressure.

2.2.3 Characterization

2.2.3.1 Mechanical properties

The mechanical properties were evaluated using Shimadzu Autograph AG-I series universal testing machine at a crosshead speed of 50 mm/min. Tensile strength, elongation at break and elastic modulus were measured according to ASTM D-882 (2002). Averages of at least five sample measurements were taken to represent each data point.

2.2.3.2 Melt Flow Index (MFI)

The melt flow index (MFI) of each blend of LDPE with filler was measured using a CEAST Modular Line Melt Flow Indexer in accordance with ASTM method D-1238 using a 2.16 kg load at a melt temperature of 190 °C.

2.2.3.3 Biodegradation studies

The biodegradation studies on the blends were carried out according to ASTM D-6691. Bacterial cultures were obtained from culture collections of *Microbial Genetic Lab, Department of Biotechnology, Cochin University of Science and Technology*. These cultures were isolated from sediment samples collected from different locations in Cochin backwaters and Mangalavanam mangroves. These cultures were previously identified as the genus *Vibrionacea* based on their morphological and biochemical characteristics outlined in Bergey's Manual of Systematic Bacteriology [Rosa et al, 2009]. They were preserved in 10mL glass bottles employing the paraffin oil overlay method.

To prepare the inoculum the individual isolates of the consortium were grown overnight at 37 °C at 120 rpm on an Orbitek shaker (Scigenics Pvt. Ltd, Chennai, India) in nutrient broth (Himedia, Mumbai) pH 7.0 ± 0.3 with 1% NaCl. The cells were harvested by centrifugation at 5000 rpm (2292 g) for 20 minutes, washed with physiological saline and then pooled. 5mL of this pooled culture (OD_{660} = 1) was used to inoculate 50mL amylase minimal medium [Roy et al, 2009] lacking starch. The samples prepared from the blends previously wiped with 70% alcohol were added to this medium and these strips acted as the sole source of carbon. Incubation was in the Orbitek environmental shaker at 37 °C and 120 rpm for a total period of 3 months with regular sampling. The medium without the inoculum with corresponding starch-plastic blends and subjected to the same treatment as above were used as controls.

2.2.3.4 Soil burial test

The soil burial test was also carried out to evaluate the biodegradability of the blends. The soil was taken in pots and the plastic strips were placed in it. The bacterial culture was supplied to the soil. Care was taken to ensure that the samples were completely covered with soil. The pot was then kept at room temperature. The loss in weight and tensile strength was measured after thorough washing with water and drying in an oven until constant weight to determine the extent of biodegradability.

2.2.3.5 Photodegradation by UV rays

In the present study, the plastic film samples were cut to 8x1 cm size and exposed under a 30-watt shortwave UV lamp at a distance of 30 cm. The plastic films were then taken out after one month to determine tensile strength using a universal testing machine. Average weight of the test specimens, before and after the degradation studies were carried out using a Sartorius-0.1 mg electronic balance. The FTIR and DSC were used for the characterization and monitoring of the functional group changes in the samples during irradiation.

2.2.3.6 Water absorption characteristics

Water absorption was measured using 3 x 1 inch film strips of <1mm thickness according to ASTM D-570-81 method. Water absorption measurements were performed by soaking the samples in distilled water. The water absorption was calculated as the weight difference and is reported as a percentage increase of the initial weight. The results reported are average of three measurements.

2.2.3.7 Fourier transform infrared spectroscopy (FTIR)

The FTIR spectra of the samples were recorded in the transmittance mode using a Thermo Nicolet, Avatar 370 FTIR spectrophotometer in the spectral range of 4000–400 cm^{-1}.

2.2.3.8 Dynamic mechanical analysis (DMA)

Dynamic Mechanical Analyzer (DMA Q-800, TA instruments) was used to study the viscoelastic properties of the samples. DMA analysis was conducted at a constant frequency of 1 Hz. A temperature ramp was run from 40 °C to 100 °C to get an overview of the thermomechanical behaviour of the samples. The dynamic storage modulus, loss modulus and tan δ were measured.

2.2.3.9 Thermogravimetric analysis (TGA)

Thermogravimetric analysis was carried out in a TGA Q-50 thermal analyzer (TA Instruments) under a nitrogen atmosphere. The samples were heated from room temperature to 600 °C at a heating rate of 20 °C/min and a nitrogen gas flow rate of 40-50 cm^3/min. The sample weights varied from 10-15 mg. The weight changes were noted with the help of an ultra sensitive microbalance. The data of weight loss versus temperature and time were recorded online using the TA Instrument's Q Series Explorer software. The analysis of the thermogravimetric (TG) and derivative thermogravimetric (DTG) curves was done using TA Instrument's Universal Analysis 2000 software version 3.3 B. The temperature at which weight loss is maximum (T_{max}) was evaluated.

2.2.3.10 Differential scanning calorimetry (DSC)

The crystallinity of the samples was studied using a TA Q-100 thermal analyzer (TA Instruments) under nitrogen atmosphere with a heating rate of 10 °C/min. Samples of 5-10 mg were heated in a nitrogen atmosphere from -50 °C to 150 °C and kept at 150 °C for 3 min to erase the thermal history. Then a cooling was performed from 150 °C to -50 °C, followed by a second heating from -50 °C to 150 °C at the same rate. The percentage of crystallinity was calculated from the DSC traces as follows.

% Crystallinity = ($\Delta H_{f\,(obs)}$ / $\Delta H_{f\,(100\%\ crystalline)}$) x 100
where $\Delta H_{f\,(obs)}$ is the enthalpy associated with melting of the material and $\Delta H_{f\,(100\%\ crystalline)}$ is the enthalpy of 100% crystalline polyethylene reported in the literature to be 286.7J/g.

2.2.3.11 Morphological studies

In the present study the tensile fractured surfaces were mounted on a metallic stub with the help of a silver tape and conducting paint in the upright position and were sputter coated with platinum within 24 hours of fractures in a JFC 1600 Autofine coater and then examined under JEOL model JSM-6390LV scanning electron microscope (SEM).

3. RESULTS AND DISCUSSION

3.1 Mechanical properties

Figure 1 illustrates the mechanical properties of pure LDPE, LDPE-starch-(EMA-Zn) blend, and blends incorporating metal oxides as pro-oxidants.

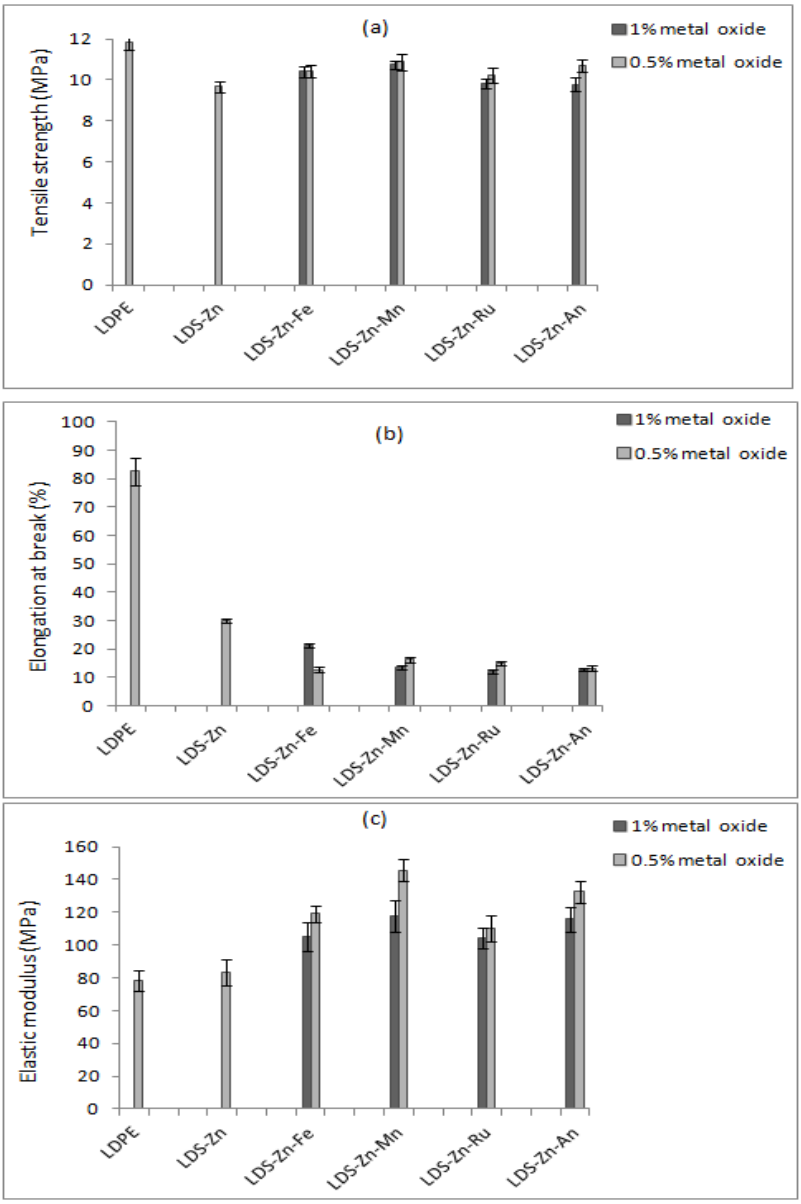

Figure 1. **Effect of metal oxides on the mechanical properties of LDPE-starch-(EMA-Zn) blends**

One key mechanical parameter assessed is the tensile strength of these materials, which denotes the maximum stress a material can withstand when subjected to pulling forces without fracturing. Notably, the figures reveal that the samples containing metal oxides exhibit tensile strength values within a comparable range to that of the pristine LDPE. This observation holds true for LDPE-starch-(EMA-Zn) blends. This suggests that the incorporation of metal oxides, which serve as pro-oxidants, has not led to a noteworthy decline in tensile

strength. This is significant because it indicates that the processing techniques and the presence of metal oxides have not induced premature degradation reactions within the materials [Ferreira, 2009].

However, in terms of elongation at break, a different trend emerges. The materials with metal oxide additives exhibit a notable reduction in elongation at break compared to the neat LDPE. This suggests that the incorporation of metal oxides impairs the material's ability to stretch before fracture. This finding could be associated with changes in the material's structure, such as increased crosslinking or alterations in polymer chain mobility, due to the presence of metal oxides.
Additionally, Figure 1(c) shows an increase in the elastic modulus of the blends containing metal oxides. The elastic modulus represents a material's stiffness and resistance to deformation under an applied load. In this context, the results indicate that all blend compositions, including those with metal oxides, possess higher elastic moduli than pure LDPE. This points to an increase in stiffness across the blends [Burjupati, 2020].

3.2 Melt flow measurements

Figure 2 shows the effect of metal oxides on the melt flow indices of LDPE-starch-(EMA-Zn) blends. The melt flow index (MFI) is a measure of a polymer's flowability under heat and pressure, indicating how easily it can be processed. A higher MFI indicates a greater ability to flow. Conversely, a lower MFI implies higher viscosity and reduced flowability.

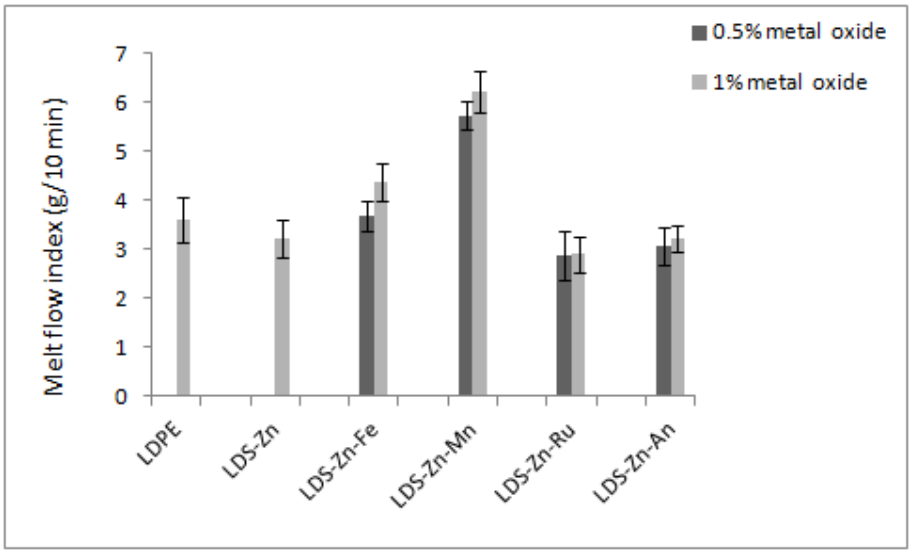

***Figure 2*. Effect of metal oxides on the melt flow indices of LDPE-starch-(EMA-Zn) blends**

For most samples of LDPE-starch-(EMA-Zn) blends containing metal oxides, the MFI values are quite similar to the MFI of pure LDPE. This observation suggests that the inclusion of these metal oxides as pro-oxidants during processing does not lead to significant chain scission (breaking of polymer chains) or crosslinking (joining of polymer chains) that would cause a substantial change in the melt flow indices. This is indicative of a controlled processing environment where the pro-oxidants do not induce major structural changes in the polymer matrix.
The exception to this trend is found with Fe_2O_3 (iron oxide) and MnO_2 (manganese dioxide) additives. In LDPE-starch-(EMA-Zn) blends incorporating Fe_2O_3 and MnO_2, the MFI values increase significantly. This increase signifies notable chain scission occurring within the polymer chains. Chain scission often results in a decrease in molecular weight, leading to a higher flowability under heat.
This variation in behavior could be attributed to the specific interactions between the metal oxides and the polymer matrix. Different metal oxides may catalyze reactions to differing extents, leading to distinct levels of chain scission or crosslinking. Reference [Kushwaha, 2023] likely offers further insights into the underlying mechanisms driving these observations, possibly discussing the chemical and physical interactions between metal oxides and the polymer blend constituents.

3.3 Biodegradation studies

Figure 3 presents the tensile characteristics of LDPE-starch-(EMA-Zn)-metal oxide blends. These blends underwent a two-month biodegradation process within a culture medium. Additionally, Table 2 provides information about the percentage decrease in tensile strength observed in these blends.

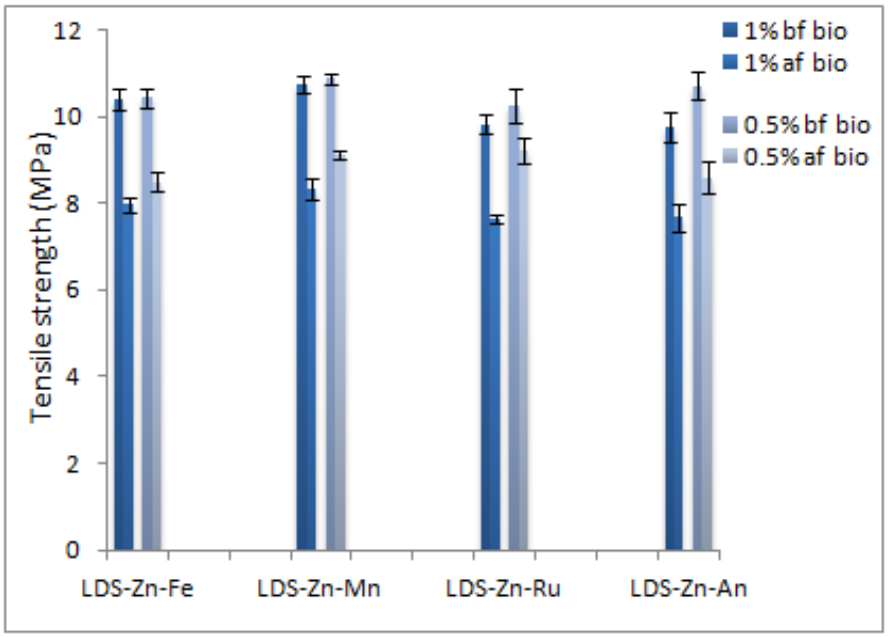

***Figure 3*. Biodegradation of LDPE-starch-(EMA-Zn)-metal oxide blends after immersion of plastic strips in culture medium for two months (Evident from tensile strength)**

***Table 2*. Percentage decrease in tensile strength of LDPE-starch-(EMA-Zn)-metal oxide blends after biodegradation in culture medium for two months**

Sample	Initial tensile strength (MPa)	Tensile strength after biodegradation for two months (MPa)	% decrease in tensile strength
LDS-Zn(1)Fe*	10.4 + 0.24	7.96 + 0.15	23.46
LDS-Zn(0.5)Fe	10.4 + 0.32	8.50 + 0.23	18.29
LDS-Zn(1)Mn	10.7 + 0.20	8.32 + 0.26	22.24
LDS-Zn(0.5)Mn	10.9 + 0.41	9.11 + 0.09	16.42
LDS-Zn(1)Ru	9.8 + 0.21	7.65 + 0.10	22.11
LDS-Zn(0.5)Ru	10.2 + 0.38	9.21 + 0.30	9.71
LDS-Zn(1)An	9.77 + 0.35	7.68 + 0.32	21.39
LDS-Zn(0.5)An	10.7 + 0.31	8.58 + 0.37	19.81

* Number given in parenthesis denotes the weight percentage of metal oxides in the blend

The biodegradation process led to a significant reduction in the tensile strength of blends [Ali et al, 2018]. This outcome is evident from the figures, which visually depict the change in tensile properties after the biodegradation period. The main factor driving this reduction is the microbial consumption of starch present in the blends. The interaction between microbes and the starch component results in its degradation, leading to a weakening of the overall structure and subsequently causing a decline in tensile strength.

The information from Table 2 offers a quantitative perspective on the extent of tensile strength decrease for the blends following biodegradation. These data add a more precise measurement to the understanding of how the blends' mechanical properties were affected.

Moreover, weight loss is highlighted as a crucial factor in assessing the biodegradation of polymers. Table 3 consolidates information on the percentage weight loss experienced by the blends after the biodegradation process in the culture medium. The results of these tables underscore the extent of degradation that occurred during the biodegradation period. The considerable weight loss across all samples after exposure to the culture medium indicates that the LDPE-starch-(EMA-Zn) blends containing metal oxides are indeed partially biodegradable.

***Table 3*. Percentage decrease in weight of LDPE-starch-(EMA-Zn)-metal oxide blends after biodegradation in culture medium for two months**

Sample	Initial weight (g)	Weight after two months (g)	% weight loss
LDS-Zn(1)Fe	0.5583	0.5434	2.666
LDS-Zn(0.5)Fe	0.5684	0.5547	2.402
LDS-Zn(1)Mn	0.6881	0.6720	2.334
LDS-Zn(0.5)Mn	0.6480	0.6332	2.283

LDS-Zn(1)Ru	0.5246	0.5150	1.824
LDS-Zn(0.5)Ru	0.5099	0.5003	1.703
LDS-Zn(1)An	0.5803	0.5710	1.613
LDS-Zn(0.5)An	0.6611	0.6511	1.505

3.4 Photodegradation studies

Figure 4 depicts the tensile characteristics of LDPE-starch-(EMA-Zn)-metal oxide blends, following one month of exposure to ultraviolet (UV) light. Complementing these figures, Table 4 provides specific information about the percentage decrease in tensile strength of blends due to UV exposure.

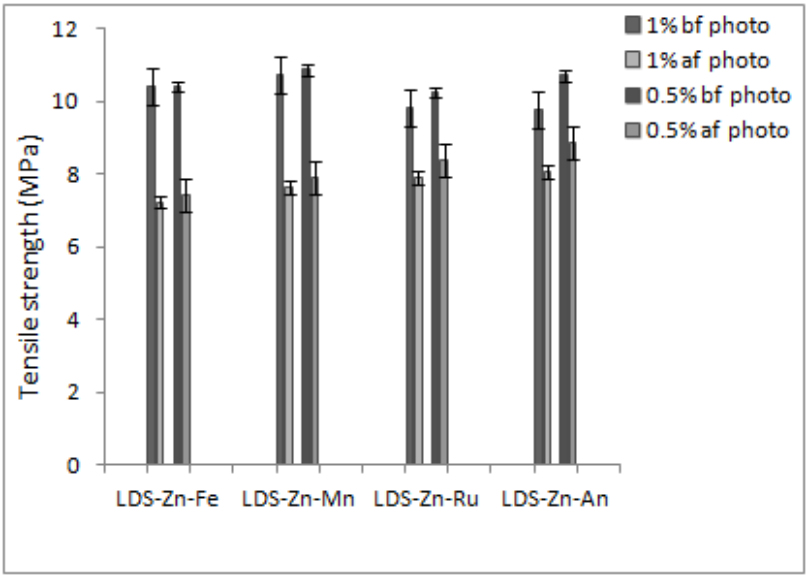

***Figure 4*. Photodegradation of LDPE-starch-(EMA-Zn)-metal oxide blends after UV exposure for one month (Evident from tensile strength)**

***Table 4*. Percentage decrease in tensile strength of LDPE-starch-(EMA-Zn)-metal oxide blends after UV exposure for one month**

Sample	Initial tensile strength (MPa)	Tensile strength after UV exposure for one month (MPa)	% decrease in tensile strength
LDS-Zn(1)Fe	10.4 + 0.24	7.23 + 0.32	30.48
LDS-Zn(0.5)Fe	10.4 + 0.32	7.43 + 0.15	28.52
LDS-Zn(1)Mn	10.7 + 0.20	7.66 + 0.26	28.41
LDS-Zn(0.5)Mn	10.9 + 0.41	7.91 + 0.11	27.41
LDS-Zn(1)Ru	9.8 + 0.21	7.92 + 0.13	19.35
LDS-Zn(0.5)Ru	10.2 + 0.38	8.39 + 0.17	17.75
LDS-Zn(1)An	9.77 + 0.35	8.05 + 0.16	17.61
LDS-Zn(0.5)An	10.7 + 0.31	8.87 + 0.28	17.22

A clear pattern emerges from the figure and table, as the tensile strength of blends undergoes a significant reduction after one month of UV light exposure. This effect is supported by the quantified data provided in the table, revealing the extent of tensile strength decrease.

UV exposure leads to changes in the chemical structure of the blends. Specifically, the polymer chains undergo modifications, resulting in the creation of new functional groups within the polymer structure. This phenomenon is particularly prominent in the amorphous regions of the material. The introduction of these new groups can influence the mechanical properties of the blends. In this case, the observed decrease in tensile strength can be attributed to these chemical changes induced by UV exposure.

***Table 5*. Percentage decrease in weight of LDPE-starch-(EMA-Zn)-metal oxide blends after UV exposure for one month**

Sample	Initial weight (g)	Weight after one month (g)	% weight loss
LDS-Zn(1)Fe	0.5690	0.5668	0.387
LDS-Zn(0.5)Fe	0.6007	0.5990	0.283
LDS-Zn(1)Mn	0.5680	0.5662	0.317
LDS-Zn(0.5)Mn	0.6657	0.6639	0.270

LDS-Zn(1)Ru	0.5197	0.5185	0.231
LDS-Zn(0.5)Ru	0.6196	0.6185	0.178
LDS-Zn(1)An	0.5319	0.5309	0.188
LDS-Zn(0.5)An	0.6676	0.6667	0.135

Furthermore, Table 5 provides insight into the weight loss experienced by the LDPE-starch-(EMA-Zn)-metal oxide blends following one month of UV exposure. The data reveal that all the samples undergo a slight decrease in weight after photodegradation. Moreover, weight loss is found to increase as the concentration of metal oxides in the blends increases. This information suggests that the presence of metal oxides could influence the susceptibility of the blends to UV-induced degradation.

3.5 Photobiodegradation studies

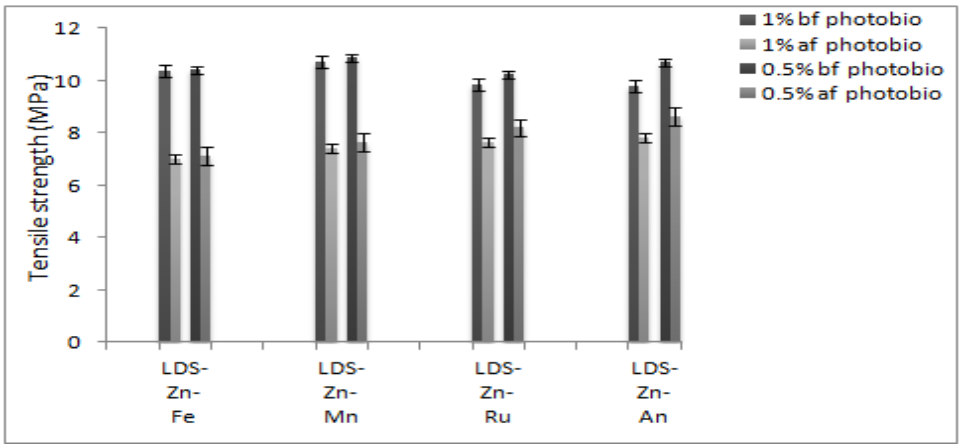

Figure 5. **Variation in tensile strength of LDPE-starch-(EMA-Zn)-metal oxide blends after UV exposure for one month followed by biodegradation in culture medium for one month**

Figure 5 showcases the tensile properties of LDPE-starch-(EMA-Zn)-metal oxide blends. The blends underwent photobiodegradation experiments, involving a two-step process: exposure to UV light for one month, followed by immersion in culture media containing amylase-generating vibrios isolated from the marine benthic environment for an additional month. Table 6 provides details about the percentage decrease in tensile strength of blends after the photobiodegradation process.
The results in Figure 5 highlight a substantial reduction in the tensile strength of the blends following two months of photobiodegradation. The data from Table 6 quantify this reduction in tensile strength, further underscoring the extent of the change.

Table 6. **Percentage decrease in tensile strength of LDPE-starch-(EMA-Zn)-metal oxide blends after photobiodegradation**

Sample	Initial tensile strength (MPa)	Tensile strength after photobiodegradation for two months (MPa)	% decrease in tensile strength
LDS-Zn(1)Fe	10.4 + 0.24	7.01 + 0.18	32.58
LDS-Zn(0.5)Fe	10.4 + 0.32	7.12 + 0.35	31.59
LDS-Zn(1)Mn	10.7 + 0.20	7.43 + 0.19	30.54
LDS-Zn(0.5)Mn	10.9 + 0.41	7.66 + 0.43	29.75
LDS-Zn(1)Ru	9.8 + 0.21	7.66 + 0.18	21.99
LDS-Zn(0.5)Ru	10.2 + 0.38	8.21 + 0.41	19.82
LDS-Zn(1)An	9.77 + 0.35	7.83 + 0.36	19.88
LDS-Zn(0.5)An	10.7 + 0.31	8.64 + 0.41	19.22

Table 7. **Percentage decrease in weight of LDPE-starch-(EMA-Zn)-metal oxide blends after photobiodegradation for two months**

Sample	Initial weight (g)	Weight after two months (g)	% weight loss
LDS-Zn(1)Fe	0.5690	0.5572	2.074
LDS-Zn(0.5)Fe	0.6007	0.5915	1.532
LDS-Zn(1)Mn	0.5680	0.5592	1.550
LDS-Zn(0.5)Mn	0.6657	0.6562	1.427
LDS-Zn(1)Ru	0.5319	0.5238	1.523
LDS-Zn(0.5)Ru	0.6676	0.6601	1.123
LDS-Zn(1)An	0.5197	0.5141	1.078
LDS-Zn(0.5)An	0.6196	0.6133	1.017

The photobiodegradation process involves a synergy between UV exposure and microbial activity. The exposure to UV light initiates a photo-oxidation process within the pro-oxidant-containing polyethylene-starch-(EMA-Zn) blends. This process leads to the formation of oxidation products and an increase in the low molecular weight fraction due to chain scission. As a result, the blends become more susceptible to biodegradation [Rosa et al, 2009].
Additionally, Table 7 details the percentage weight loss observed in the blends after undergoing biodegradation in the culture medium. Following photobiodegradation, all samples experience a significant loss in weight. This weight loss is attributed to the microbial breakdown of the oxidation products formed during the photobiodegradation process. Microbes utilize these oxidation products as a substrate, leading to the observed weight loss.

3.6 Water absorption studies

Percentage water absorption tests were conducted to assess the hydrophilicity level of LDPE-starch-(EMA-Zn)-metal oxide blends. In this context, Table 8 provides an overview of the water absorption characteristics exhibited by these composites. The goal of this test is to determine the extent to which water is absorbed by the blends, indicating their propensity to interact with and absorb moisture [Maziad, 2021].

Table 8. **Water absorption of LDPE-starch-(EMA-Zn)-metal oxide blends**

Sample	Initial weight (g)	Weight after 24 hours (g)	% water absorption
LDS-Zn(1)Fe	0.3552	0.3596	1.239
LDS-Zn(0.5)Fe	0.3045	0.3082	1.215
LDS-Zn(1)Mn	0.2764	0.2799	1.27
LDS-Zn(0.5)Mn	0.4014	0.406	1.146
LDS-Zn(1)Ru	0.5558	0.5624	1.188
LDS-Zn(0.5)Ru	0.3295	0.3330	1.062
LDS-Zn(1)An	0.4321	0.4372	1.180
LDS-Zn(0.5)An	0.3741	0.3780	1.043

Table 9. **Water absorption of LDPE-starch-(EMA-Zn) blends**

Sample	Initial weight (g)	Weight after 24 hours (g)	% water absorption
LDS(0)-Zn(2)	0.2999	0.3001	0.07
LDS(0)-Zn(5)	0.2537	0.2538	0.04
LDS(15)-Zn(2)	0.2432	0.2453	0.86
LDS(15)-Zn(5)	0.2996	0.3016	0.67
LDS(20)-Zn(2)	0.3722	0.3771	1.32
LDS(20)-Zn(5)	0.4332	0.4387	1.27
LDS(30)-Zn(2)	0.3080	0.3156	2.47
LDS(30)-Zn(5)	0.4317	0.4373	1.30
LDS(40)-Zn(2)	0.3721	0.3870	4.00
LDS(40)-Zn(5)	0.4072	0.4201	3.17

(LDS(0)-Zn(2) = LDPE- 0%starch-2% EMA-Zn; LDS(0)-Zn(5) = LDPE- 0%starch-5% EMA-Zn; LDS(15)-Zn(2) = LDPE- 15%starch-2% EMA-Zn; LDS(15)-Zn(5) = LDPE- 15%starch-5% EMA-Zn; LDS(20)-Zn(2) = LDPE-20%starch-2% EMA-Zn; LDS(20)-Zn(5) = LDPE- 20%starch-5% EMA-Zn; LDS(30)-Zn(2) = LDPE-30%starch-2% EMA-Zn; LDS(30)-Zn(5) = LDPE- 30%starch-5% EMA-Zn; LDS(40)-Zn(2) = LDPE-40%starch-2% EMA-Zn; LDS(40)-Zn(5) = LDPE- 40%starch-5% EMA-Zn)

The data in Table 9 reveal that the presence of metal oxides in the blends does not lead to any significant alteration in their water absorption behavior, when compared to the blends without metal oxides. This implies that the addition of metal oxides does not notably affect the blends' overall capacity to absorb water.

Additionally, the data point out a distinct trend in water absorption among the various compositions. Specifically, when considering films containing 1% metal oxides in EMA-Zn compatible blends, the percentage water absorption follows a specific order: LDS-(1)Fe > LDS-(1)Mn > LDS-(1)Ru > LDS-(1)An. This sequence signifies that the blend containing iron oxide (Fe) exhibits the highest water absorption rate, followed by manganese dioxide (Mn), rutile-grade titanium dioxide (Ru), and anatase-grade titanium dioxide (An). This information provides insights into how different metal oxides impact the hydrophilicity of the blends.

3.7 FTIR spectroscopy

The FTIR spectra of the LDPE-starch-(EMA-Zn)-Fe_2O_3 films before and after biodegradation are shown in Figure 6. The spectrum of the LDPE-starch-(EMA-Zn)-Fe_2O_3 film exhibits distinctive absorption peaks, as shown in Table 10. Peaks at 2921-2848 cm^{-1}, 1473-1463 cm^{-1}, and 730-720 cm^{-1} are caused by symmetrical stretching vibration of C-H bonds, bending vibration of C-H bonds, and crystalline and amorphous band absorption.

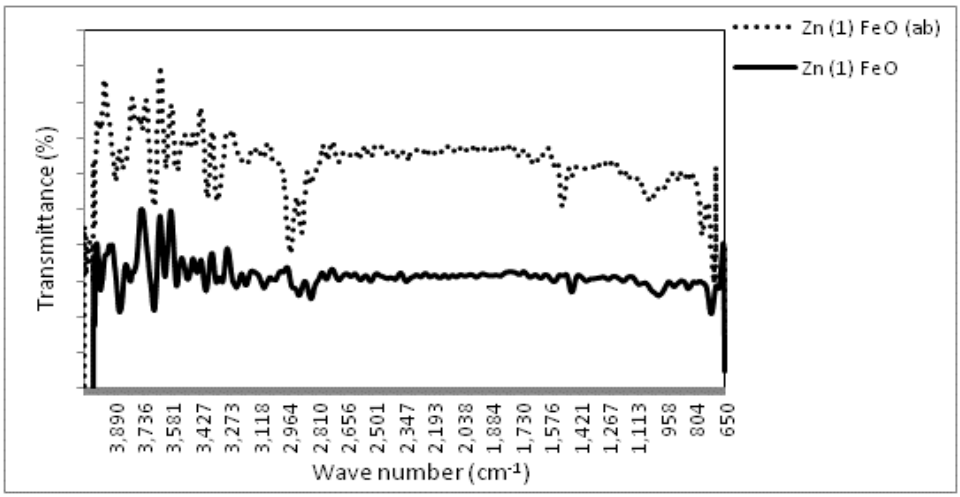

Figure 6. **FTIR spectra of LDPE-starch-(EMA-Zn)-Fe2O3 blend: (-) before biodegradation and (...) after biodegradation**

Table 10. **Characteristic FTIR spectral peaks**

Sample	Peak position (cm^{-1})	Characteristic group
LDPE- starch-(EMA-Zn)-Fe_2O_3 film	2911, 2845	C-H stretching
	1557	C=O stretching
	1461	CH_2 scissor and asymmetric bending
	1368	C-H bending
	1001	O-C stretching
	932	O-H deformation
	721	CH_2 rocking

Peak intensities of films at 2921-2848 cm^{-1}, 1473-1463 cm^{-1}, 1156-1028 cm^{-1}, and 730-720 cm^{-1} were all considerably enhanced after two months of biodegradation in culture, as seen in the figure. The rise in peak intensity is due to polyethylene chain fracture in degradable conditions, which resulted in an increase in terminal group numbers. Furthermore, the carbonyl group generated by polyethylene oxidation caused the peak at 1706 cm^{-1} after decomposition.

The peaks at 1156 cm^{-1} and 1028 cm^{-1} are attributable to starch C-O-C bond stretching, while the peak near 1001 cm^{-1} is the anhydroglucose ring O-C stretch. The breakdown of starch increased the intensity of these peaks, indicating that the inclusion of ferric oxide had no negative impact on the biodegradation of LDPE-starch-(EMA-Zn) blends.

3.8 Dynamic mechanical analysis

Figure 7 provides graphical representations of the changes in storage modulus observed in LDPE-starch-(EMA-Zn) blends that incorporate metal oxides. These measurements were taken over a temperature range spanning from 40°C to 100°C. The storage modulus is a measure of a material's ability to store and return energy under deformation, representing its stiffness or resistance to deformation.

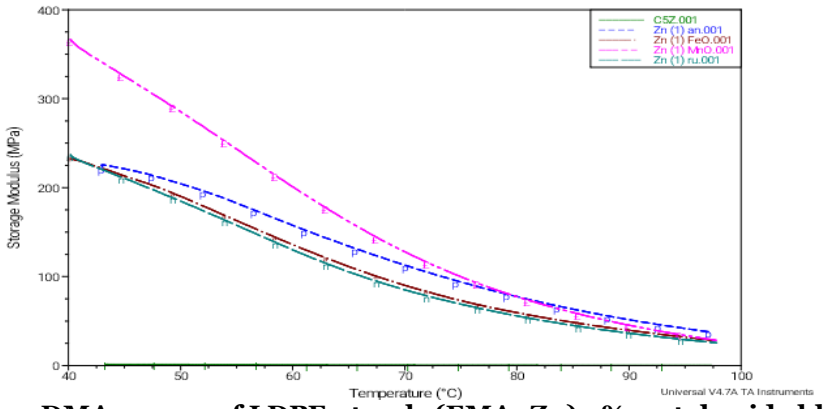

Figure 7. **DMA curves of LDPE-starch-(EMA- Zn)-1% metal oxide blends**

The key observation drawn from these figures is that the presence of metal oxides in the blends led to an increase in the values of the storage modulus. This upward shift in the storage modulus values indicates an enhancement in the stiffness and rigidity of the blends. Essentially, the materials became less deformable in response to applied forces.

This change in stiffness can be attributed to an improvement in the interfacial contact between the different phases present within the blends. In polymer blends, different components often have different properties, and achieving good interfacial adhesion is essential for maintaining the integrity of the material. The introduction of metal oxides appears to have contributed to a stronger interfacial interaction, which, in turn, led to higher storage modulus values [Bulatovic, 2021].

3.9 Thermogravimetric analysis (TGA)

Figure 8 depicts thermograms of LDPE-starch-(EMA-Zn)-1% metal oxide blend. These thermograms offer insights into the thermal breakdown behavior of these blends under increasing temperature conditions [Estrada-Monje et al, 2021].

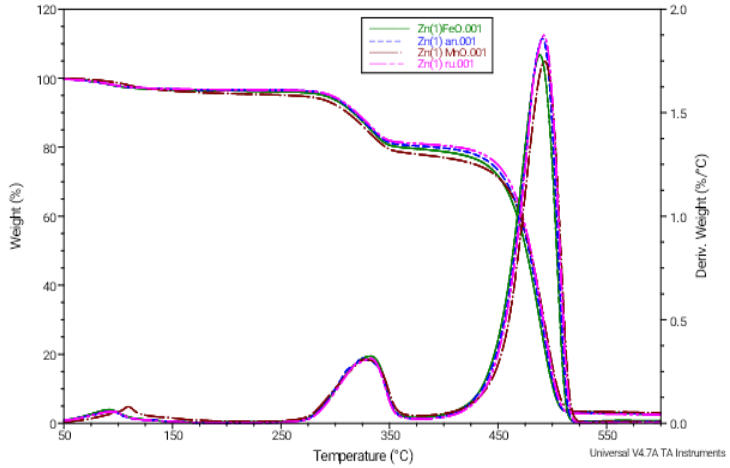

Figure 8. **TGA thermograms of LDPE-starch-(EMA-Zn)-1% metal oxide blends**

The thermograms show distinct regions of weight loss, each corresponding to specific thermal degradation processes.

1. First weight loss region (Approximately 100°C): This initial weight loss region can be attributed to the thermal degradation of low molecular weight constituents within the blend. These are likely components with lower molecular weight and weaker bonds that undergo thermal breakdown at relatively lower temperatures.
2. Second weight loss region (225°C-350°C): The weight loss observed in this region can be linked to the thermal breakdown of starch within the blend. Starch is a polysaccharide that can degrade when exposed to elevated temperatures. The thermal degradation of starch could result in the release of volatile compounds and the reduction in the overall mass of the blend.
3. Third weight loss region (420°C-525°C): This weight loss region is attributed to the thermal degradation of the backbone chains of pure polyethylenes. The main structural components of polyethylene chains undergo thermal breakdown at these higher temperatures.

Table 11. **TGA results for LDPE-starch-(EMA-Zn)-1% metal oxide blends**

Sample	Temperature of onset of degradation (°C)	T_{max} (°C)	Rate of maximum degradation (%/°C)	Residual weight (%)
LDS-Zn	431.28	490.07	2.082	1.209
LDS-Zn(1)Fe	421.57	488.53	1.779	2.417
LDS-Zn(1)An	424.32	490.88	1.857	2.603

Table 11 presents summarized thermogravimetric parameters for the different blends, providing a quantitative perspective on their thermal stability. The data suggest that the presence of metal oxides in LDPE-starch-(EMA-Zn) composites leads to a reduction in their thermal stability. In other words, the blends containing metal oxides tend to degrade at lower temperatures compared to those without metal oxides.
This decrease in thermal stability could be attributed to interactions between the metal oxides and the polymer matrix. These interactions might promote degradation pathways or accelerate the breakdown of polymer chains under thermal stress.
The insights provided by this information contribute to understanding how the presence of metal oxides impacts the thermal behavior of LDPE-starch-(EMA-Zn) blends. This has implications for the stability and performance of these materials under different temperature conditions.

3.10 Differential scanning calorimetry (DSC)

Table 12 along with Figure 9, provide insights into the thermal behavior of LDPE-starch-(EMA-Zn)-ferric oxide (74/20/5/1) blend both before and after undergoing biodegradation. These elements contribute to understanding how the presence of ferric oxide impacts the thermal properties of the blends and how these properties change as a result of biodegradation.

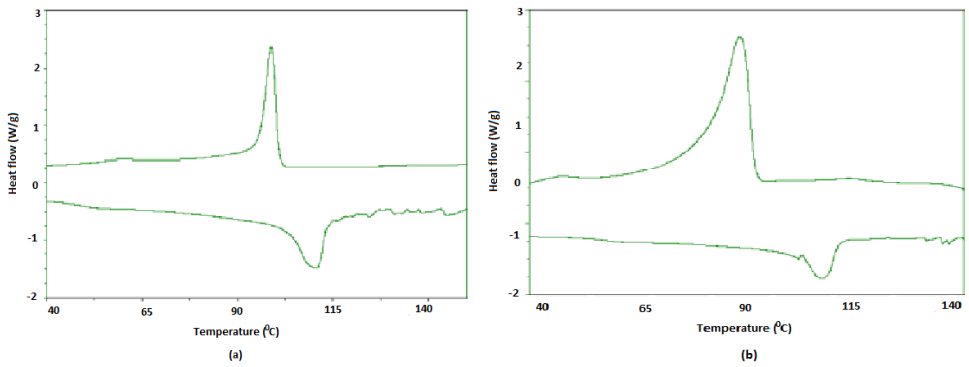

Figure 9. **DSC curves of LDPE-starch-(EMA- Zn)-1% ferric oxide blend: a) before biodegradation and b) after biodegradation**

The data in the table reveal that the addition of ferric oxide does not have any significant effect on the melting temperature (T_m) of pure LDPE. This suggests that the presence of ferric oxide does not alter the overall crystalline structure of LDPE, at least in terms of its melting behavior. The melting temperature is a key indicator of the crystalline arrangement of a polymer.

Table 12. **Results of DSC analysis of LDPE-starch-(EMA-Zn)-1% ferric oxide blend**

Sample	Tm (oC)	ΔHf (J/g)	Tc (oC)	ΔHc (J/g)	% crystallinity
LDPE	110.00	67.00	96.00	79.00	23.4
LDS-Zn(1)Fe	110.50	49.83	98.82	54.55	17.4
LDS-Zn(1)Fe(ab)	110.91	24.14	93.51	53.89	8.4

For the LDPE-starch-(EMA-Zn)-ferric oxide blend, the incorporation of ferric oxide leads to a reduction in the crystallinity of LDPE. This decrease in crystallinity is likely related to the presence of an amorphous phase in the blend. The amorphous phase lacks the well-defined, ordered structure of the crystalline phase. This reduction in crystallinity could be significant because it may have contributed to the biodegradation process.
The decrease in crystallinity observed after two months of biodegradation is likely connected to the changes occurring during degradation, particularly in the amorphous phase of the polymer. Amorphous regions are generally more susceptible to degradation due to the lack of a highly ordered structure that provides stability.
The early alterations associated with degradation tend to manifest in the amorphous phase of the polymer first. As a result, the decrease in crystallinity observed could be indicative of changes taking place within the amorphous regions as a consequence of biodegradation [Ramírez-Hernández et al, 2020].

3.11 Morphological studies

Figure 10 in the study displays scanning electron micrographs showcasing the cracked surfaces of an LDPE-starch-(EMA-Zn) blend that incorporates 1% ferric oxide. The micrographs depict the material before and after undergoing two months of biodegradation in a culture medium. These images provide visual evidence of how the presence of ferric oxide and the biodegradation process impact the surface morphology of the blend [Saeed, 2022].

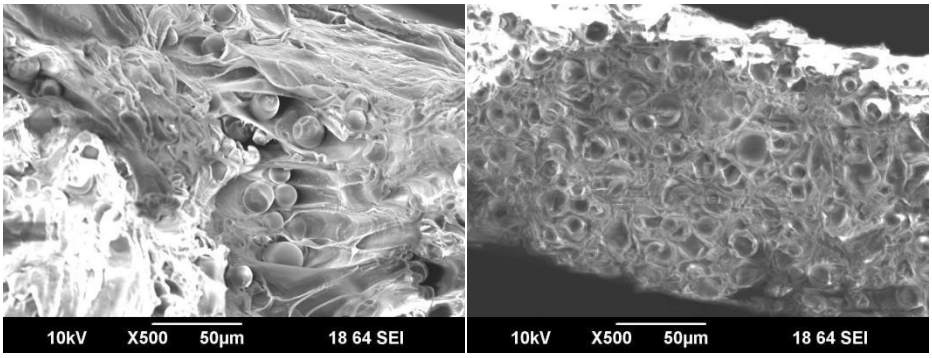

(a)

(b)

Figure 10. **Scanning electron micrographs of LDPE-starch-(EMA-Zn) blend containing 1% Fe_2O_3 as pro-oxidant:**

(a) before biodegradation and (b) after biodegradation for two months

After the two-month biodegradation period, the micrographs reveal the presence of numerous tiny cavities on the LDPE-starch-(EMA-Zn)-ferric oxide blend surface. This observation indicates that microorganisms have effectively eliminated starch from the blend. The presence of cavities is a result of the microbial action on the starch component. Interestingly, in the case of the ferric oxide-incorporated blend, the number of cavities is fewer compared to the LDPE-starch blend as depicted in figure 11. This suggests that the inclusion of ferric oxide has some impact on limiting the extent of starch removal by microorganisms.

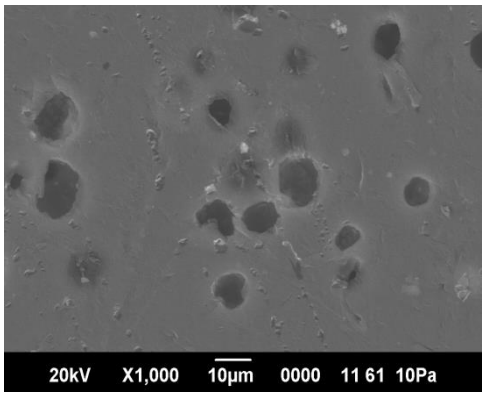

Figure 11. **Scanning electron photo-micrograph of LDPE-starch blend after biodegradation in culture medium for eight weeks**

The improved preservation of starch in the ferric oxide-incorporated blend might be due to the interaction between ferric oxide and the polymer matrix. This interaction could potentially hinder microbial access to the starch, slowing down its degradation. Additionally, the presence of the compatibilizer (EMA-Zn) appears to play a role in enhancing the interfacial adhesion of the blend samples containing ionomer. This improvement in interfacial adhesion could contribute to the better preservation of the material's structure and components during biodegradation.

4. CONCLUSION

The incorporation of modest amounts of metal oxides (ferric oxide, manganese dioxide, titanium dioxide (rutile and anatase grades)) in EMA-Zn (5%) compatibilized low density polyethylene-starch blends resulted in minor modifications in LDPE mechanical properties. The addition of tiny amounts of titanium dioxide (rutile and anatase grades) resulted in a minor change in the melt flow index of LDPE. However, the addition of trace amounts of ferric oxide and manganese dioxide increases the melt flow index of LDPE. The tensile strength of all samples decreased significantly following immersion in the culture medium, demonstrating biodegradation of the blends by microorganisms, as validated by IR spectroscopy.

When exposed to UV radiation, the presence of trace amounts of metal oxides causes degradation of LDPE-starch-(EMA-Zn) blends. After photobiodegradation, all of the samples showed a considerable drop in tensile strength and weight. The addition of metal oxides increased the rate of deterioration in the following order: FeO > MnO > Ru > An. The addition of tiny amounts of metal oxides raised the storage modulus in all of the samples, indicating stiffening. The addition of modest amounts of metal oxides affects LDPE's thermal stability and crystallinity. The biodegradation of the pro-oxidant-incorporated blend samples is confirmed by SEM micrographs.

CRediT authorship contribution statement. Author 1: Methodology, Investigation, Formal Analysis Author 2: Review, proof reading Author 3: Supervision.

Declaration of competing interest. The authors declare that we have no known competing financial interests or personal relationships that could have appeared to influence the work reported in this paper.

REFERENCES

1. Ali A, Xie F, Yu L, Liu H, Meng L, Khalid S, Chen L. Preparation and characterization of starch-based composite films reinfoced by polysaccharide-based crystals. Composites. Part B, Engineering, 133(2018)122–128. http://dx.doi.org/10.1016/j.compositesb.2017.09.017. doi:10.1016/j.compositesb.2017.09.017
2. Ammala A, Bateman S, Dean K, Petinakis E, Sangwan P, Wong S, Yuan Q, Yu L, Patrick C, Leong KH. An overview of degradable and biodegradable polyolefins. Progress in polymer science, 36(8)(2011)1015–1049. http://dx.doi.org/10.1016/j.progpolymsci.2010.12.002. doi:10.1016/j.progpolymsci.2010.12.002
3. Bardají DKR, Moretto JAS. João Pedro Rueda Furlan & Eliana Guedes Stehling ; A mini-review: current advances in polyethylene biodegradation, 36(2020)
4. Bonhomme S, Cuer A, Delort A-M, Lemaire J, Sancelme M, Scott G. Environmental biodegradation of polyethylene. Polymer degradation and stability, 81(3)(2003)441–452. http://dx.doi.org/10.1016/s0141-3910(03)00129-0. doi:10.1016/s0141-3910(03)00129-0
5. Buchanan RE, Gibbons NE. Bergey's manual of systematic bacteriology, 8th edn. Baltimore: The Williams and Wilkins Co.,(1974)
6. Bulatović VO, Mandić V, Kučić Grgić D, Ivančić A. Biodegradable polymer blends based on thermoplastic starch. Journal of polymers and the environment, 29(2)(2021)492–508. http://dx.doi.org/10.1007/s10924-020-01874-w. doi:10.1007/s10924-020-01874-w
7. Burelo M, Hernández-Varela JD, Medina DI, Treviño-Quintanilla CD. Recent developments in bio-based polyethylene: Degradation studies, waste management and recycling,Heliyon,9(11)(2023):e21374. http://dx.doi.org/10.1016/j.heliyon.2023.e21374. doi:10.1016/j.heliyon.2023.e21374
8. Burjupati NR, Kandiban R, Parthasarathy A. Role of metal oxide nano particles in improving electrical, dielectric and thermal properties of polyethylene nano dielectric. In: Lecture Notes in Electrical Engineering. Cham: Springer International Publishing, (2020)182–193.
9. Estrada-Monje A, Alonso-Romero S, Zitzumbo-Guzmán R, Estrada-Moreno IA, Zaragoza-Contreras EA. Thermoplastic starch-based blends with improved thermal and thermomechanical properties. Polymers, 13(23)(2021)4263. http://dx.doi.org/10.3390/polym13234263. doi:10.3390/polym13234263
10. Ferreira FGD, Lima MAGA, Almeida YMB, Vinhas GM. Evaluation of photodegradation in LDPE/modified starch blends. Polímeros, 19(4)(2009)313–317. http://dx.doi.org/10.1590/s0104-14282009000400011. doi:10.1590/s0104-14282009000400011
11. Ghatge, S., Yang, Y., Ahn, JH. et al. Biodegradation of polyethylene: a brief review. Applied Biological Chemistry, 63, 27 (2020). https://doi.org/10.1186/s13765-020-00511-3
12. Inceoglu F, Menceloglu YZ. Transparent low-density polyethylene/starch nanocomposite films. Journal of applied polymer science, 129(4)(2013)1907–1914. http://dx.doi.org/10.1002/app.38811. doi:10.1002/app.38811
13. Jiang T, Duan Q, Zhu J, Liu H, Yu L. Starch-based biodegradable materials: Challenges and opportunities. Advanced industrial and engineering polymer research, 3(1)(2020)8–18. http://dx.doi.org/10.1016/j.aiepr.2019.11.003. doi:10.1016/j.aiepr.2019.11.003
14. Kushwaha A, Goswami L, Singhvi M. Beom Soo Kim; Biodegradation of poly(ethylene terephthalate): Mechanistic insights, advances, and future innovative strategies. Chemical Engineering Journal, (2023)457

15. Maziad NA, Abdel Ghaffar AM, Ali HE. Polyethylene film modification using polylactic acid - Starch additives and study ionizing radiation effect onto aging properties. Environmental progress & sustainable energy, 40(2)(2021) http://dx.doi.org/10.1002/ep.13556. doi:10.1002/ep.13556
16. Nagwan Galal El Menofy & Abdelrahman Mossad Khattab; Plastics Biodegradation and Biofragmentation; Handbook of Biodegradable Materials, (2022)1–30.
17. Ramírez-Hernández A, Hernández-Mota CE, Páramo-Calderón DE, González-García G, Báez-García E, Rangel-Porras G, Vargas-Torres A, Aparicio-Saguilán A. Thermal, morphological and structural characterization of a copolymer of starch and polyethylene. Carbohydrate research, 488(2020)107907. http://dx.doi.org/10.1016/j.carres.2020.107907. doi:10.1016/j.carres.2020.107907
18. Rosa DS, Grillo D, Bardi MAG, Calil MR, Guedes CGF, Ramires EC, Frollini E. Mechanical, thermal and morphological characterization of polypropylene/biodegradable polyester blends with additives. Polymer testing, 28(8)(2009)836–842. http://dx.doi.org/10.1016/j.polymertesting.2009.07.006.
19. Roy PK, Surekha P, Rajagopal C, Chatterjee SN, Choudhary V. Accelerated aging of LDPE films containing cobalt complexes as prooxidants. Polymer degradation and stability, 91(8)(2006)1791–1799. http://dx.doi.org/10.1016/j.polymdegradstab.2005.11.010. doi:10.1016/j.polymdegradstab.2005.11.010
20. Roy PK, Surekha P, Raman R, Rajagopal C. Investigating the role of metal oxidation state on the degradation behaviour of LDPE. Polymer degradation and stability, 94(7)(2009)1033–1039. http://dx.doi.org/10.1016/j.polymdegradstab.2009.04.025. doi:10.1016/j.polymdegradstab.2009.04.025
21. Saeed S, Iqbal A, Deeba F. Biodegradation study of Polyethylene and PVC using naturally occurring plastic degrading microbes. Archives of microbiology, 204(8)(2022)http://dx.doi.org/10.1007/s00203-022-03081-8. doi:10.1007/s00203-022-03081-8
22. Sanniyasi E, Gopal RK, Gunasekar DK, Raj PP. Biodegradation of low-density polyethylene (LDPE) sheet by microalga, Uronema africanum Borge. Scientific reports,11(1)(2021)17233. http://dx.doi.org/10.1038/s41598-021-96315-6. doi:10.1038/s41598-021-96315-6
23. Zhang Y, Pedersen JN. Zheng Guo; Biodegradation of polyethylene and polystyrene: From microbial deterioration to enzyme discovery. Biotechnology Advances, (2022)60
24. Zhao X, Li Z, Chen Y, Shi L, Zhu Y. J Mole Cata A: Chem, 268(2007)